International Journal on Advanced Science Engineering Information Technology

Vol.8 (2018) No. 1
ISSN: 2088-5334

Modification of TiO_2 Nanotube Arrays with N Doping and Ag Decorating for Enhanced Visible Light Photoelectrocatalytic Degradation of Methylene Blue

Anthoni B. Aritonang[#], Yuni K. Krisnandi[#], Jarnuzi Gunlazuardi[#]

[#]*Department of Chemistry, Faculty of Mathematics and Science, University of Indonesia, Depok, 16424, Indonesia*
E-mail: jarnuzi@ui.ac.id, toniarios08@gmail.com

***Abstract*—The Ag/N-TiO_2 nanotube arrays photocatalyst have been successfully fabricated by in-situ anodization method and followed by calcining at 450°C under N_2 atmospheric condition. The inner diameter, wall thickness, and length of the nanotube arrays are approximately 65 nm, 15 nm, and 900 nm, respectively. Ag nanoparticles with diameter around 20-30 nm are deposited on the surface of the N-TiO_2 by an electrochemical deposition method. Compared with the TiO_2 nanotube arrays, the Ag/N-doped TiO2 showed a significant enhancement of photoelectrocatalytic (PEC) degradation on methylene blue (MB), was about 92% for 240 min under visible light irradiation. The kinetic constant of Ag/N-doped TiO_2 electrode was about 9 times higher than TiO_2. The enhanced photocatalytic activity under visible light irradiation of Ag/N-doped TiO_2 is a synergistic effect of N-doping and Ag nanoparticles deposited. Furthermore, the kinetic constant PEC degradation of MB is a contribution of photo-generated electron-hole separation efficiency, due to bias potential which was applied to the surface of the electrode. The Ag/N- TiO_2 is a promising photocatalyst for organic pollutant degradation which is visible light responsive.**

***Keywords*— nanotube arrays; anodization; electrochemical deposition; bias potential; photoelectrocatalytic**

I. INTRODUCTION

Highly ordered TiO_2 nanotube arrays have received considerable attention because of their large specific surface area to adsorptive capacity, good photocatalytic activity and chemical stability that can be exploited in applications such as solar cell [1], [2], water splitting [3], biological process [4] and environmental purification [5]. The main advantages of the unique its nanotube arrays architecture with wall thickness, which enhances the charge transport in the TiO_2-electrolyte interface [2] and extensive applications in solar light conversion. Unfortunately, TiO_2 nanotube arrays with a wide band gap (3,2 eV) can only respond to UV light irradiation, which limits their application because UV light possesses about 5% of the solar spectrum. Another problem impeding application of TiO_2 photocatalyst is that the photogenerated electron-hole pairs are easily recombined results in low photocatalytic efficiency [6].

Several attempts have been tried to improve its visible light response by nonmetal doping, such as B [7], [8], S [9], C [10] or N [11]-[13]. Among these elements, N doping into TiO_2 lattice has been demonstrated the red shift of absorption edge to the visible light region [14]. In our previous work, N-doped TiO_2 nanotube arrays were synthesized via in situ anodization method, and it was found that N doping into TiO_2 nanotube arrays lattice contributed to reduce the band gap of TiO_2 and improve the photocatalytic degradation of the methylene blue under visible light irradiation [15]. However, it is still not sufficient for the photocatalytic application, because of low photocatalytic efficiency due to high recombination photogenerated carrier. Recently, co-modification of TiO_2 using N doping and metal loading have been reported to be an efficient attempt for the photocatalytic enhancement activity [16], [17]. Decorating N-doped TiO_2 surface with a noble metal, such as Fe, Pt and Ag provide a potential to improve photocatalytic activities with high efficiency under visible light irradiation [18]. The noble metal with nanoparticles is deposited on the N-doped TiO_2 surface act as a mediator for the interfacial charge transfer and prevent the photogenerated electron-hole pairs recombination [19]. Among of the noble metals, Ag is the most preferred element because it matches with N-doped TiO_2 owing to the favorable energy level [20]. The deposition of Ag nanoparticles onto the surface of N-doped TiO_2 can markedly broaden the absorption edge to visible light region due to surface plasmon resonance (SPR) [21]. The local plasmonic resonance in Ag nanoparticles can enhance the electric fields, facilitating photogenerated electron-hole

production. Furthermore, interactions between the TiO_2 and Ag have been recognized Schottky barriers, which can facilitate to separate the photogenerated electron-hole pairs promotes interfacial electron transfer process [22]. Mingxuan et al. [23] were reported that Ag-N co-doped TiO_2 prepared by in situ calcination process. The photoelectrochemical performance is associated with an enhanced visible light response and high photogenerated electron-hole separation efficiency, due to the synergetic effect of N-doping and Ag-loading. Shenseng et al.[24] prepared Ag loaded N-doped TiO_2 by the electrochemical anodization followed electrodeposition method and found a high photocatalytic degradation efficiency for the degradation of Acid orange. Jiqing et al. [25] fabricated Ag/N-doped TiO_2 by electrochemical deposition. They suggest that the Ag nanoparticles were deposited on N-doped TiO_2 surface increasing electron transfer, which enhanced the photoelectrochemistry performance.

Most of the previously reported methods for synthesis of Ag/N co-doped TiO_2 involved multiple steps, in which the preparation of TiO_2 and N doping are occurred at different stages [23]-[25], which is complex and time-consuming. Ammonia or NH_3 as N dopant source for preparation of the N-doped TiO_2 is not environmental friendly. Furthermore, the kinetics of photocatalytic process under visible light irradiation not reported.

In this paper, we report on synthesis N-doped TiO_2 nanotube arrays by in-situ anodization followed calcining at 450^oC under N_2 atmosphere. The N-doped TiO_2 surface has been decorated with Ag nanoparticles by electrochemical deposition. The Ag/N co-doped TiO_2 are investigated by XRD, FESEM, EDX, XPS and UV-visible absorption spectra.

The photocurrent response was investigated the photoelectrochemical behaviour performance, and then photocatalytic activities are evaluated using the photoelectrocatalytic degradation of methylene blue under visible light irradiation. The effect of N-doping and Ag-decorating into TiO_2 nanotube arrays on the photoelectrocatalytic kinetics was also investigated.

II. Materials and Methods

The N-doped TiO_2 nanotube arrays (denoted N-TiO_2) were synthesized by *in-situ* anodization process according to our previous report [15]. Briefly, Ti foil (from Baoji Jinsheng Metal Material Co, purity 99.6%, the thickness of 0.3 mm) with the square area (1.0 cm x 3.0 cm) were mechanically polished with sandpapers and then degreased by sonication in acetone, ethanol and deionized water for 10 min, respectively and dried in nitrogen stream. Then the cleaned Ti substrates were anodized in the electrolyte ethylene glycol consisted of the NH_4F (0.3 wt%), deionized water (2.0 wt%) and 0.2 wt% triethylamine (1.5 $mol.L^{-1}$), in the two-electrode electrochemical cell (Ti foil as the anode and Pt foil as the cathode). The potential was controlled about 40 V for 1 h using a DC power supply. The as-prepared sample was rinsed with deionized water and subsequently calcined at 450^oC for 3 h with a heating and cooling rate of $5.0^oC\ min^{-1}$ under a nitrogen atmosphere (5.0 $mL.min^{-1}$) to induce anatase crystallization. This simple method comprised simultaneously N doping and fabricated of TiO_2 nanotube arrays. Finally, N-TiO_2 can be prepared successfully.

The Ag-decorated on N-TiO_2 surface were prepared by electrochemical deposition methods in a two-electrode cell comprised of N-TiO_2 and Pt foil used as the working and counter electrode, respectively. The working electrode was immersed in the electrolyte solution containing $AgNO_3$ solution 2.0 $g.L^{-1}$ and EDTA 0.1 $g.L^{-1}$ for 10 min in the dark before electrochemical deposition processes. The electrochemical deposition was carried out at room temperature using a potentiostat eDaQ. The deposition potential was controlled at -1.0 V and the deposition time varied for 5 to 25 s. The as-prepared samples were dried at 60^oC overnight until results the Ag/N-TiO_2.

The morphology of the obtained samples were characterized by field emission scanning electron microscope (FESEM, FEI-Inspect F50) with accelerating voltage of 20 kV.

The crystalline structure of the samples was identified by X-ray diffraction (XRD-PHILIPS PW 1710) using Cu Kα as a radiation source in the range 10-80°(2θ). The elemental composition was determined using EDX, and chemical states were analyzed by X-ray photoelectron spectroscopy (XPS, K-alpha Thermo Scientific) using a monochromatic Al Kα radiation source (15 mA, 14 kV). Diffuse reflectance spectra (DRS) of the samples were recorded by a spectrophotometer with software UV Probe (DRS-8000 Shimadzu).

The photoelectrochemical measurement was performed in 0.1 $g.L^{-1}$ KOH solution as the electrolyte using a three-electrode with the obtained samples as the working electrode, an Ag/AgCl electrode as the reference, and a platinum foil as the counter electrode. A 150 W Hollolite lamp (wavelength 425 nm, contain UV light a portion of ~10%) which provided an irradiation intensity of 37 $mWcm^{-2}$ was used as the visible light source. The photocurrent density of the sample was measured with a scanning potentiostat (eDAQ version 9.1) by linear sweep voltammogram from -1.0 V to 1.0 V at a rate of 100 mVS^{-1} under visible light irradiation.

The photocatalytic (PC) and photo electrocatalytic (PEC) activities of the obtained electrodes were evaluated by degradation of methylene blue (MB) aqueous solution with an initial concentration of 10 $mg.L^{-1}$ containing KOH 0.1 $g.L^{-1}$ as the electrolyte. The PEC process was performed in a semi-cylindrical quartz reactor (3.0 cm x 6.0 cm) using the Ag/N-TiO_2 (1.5 cm x 1.5 cm) as photoanode, Pt foil as cathode and an Ag/AgCl as the reference electrode with bias potential applied 0.5 V, and a 150 W Hollolite lamp (Philip, China) was employed as the visible light source.

The distance between the PEC reactor with the visible light source was 20 cm (intensity of 37 $mWcm^{-2}$). Prior to PEC degradation, the electrode was soaked in MB solution (10 mg L^{-1}) in the dark for 30 min to establish the adsorption-desorption equilibrium. During the PEC process, the MB concentration was analyzed at a time interval of every 10 min by measuring the absorbance using a UV-visible spectrophotometer (Shimadzu 2450). The reaction solution (~2.0 mL) was quickly withdrawn at given reaction intervals and was returned to the reactor after being analyzed.

III. Results and Discussion

The XRD patterns of TiO_2, N-TiO_2 and Ag/N-TiO_2 are shown in Fig. 1. The crystal structures for all samples gave peaks the diffraction of the field (110), (004), (200) and (204), indicating that all samples exhibit the crystalline phase of anatase, consistent with TiO_2 standards (JCPDS No.21-1272).

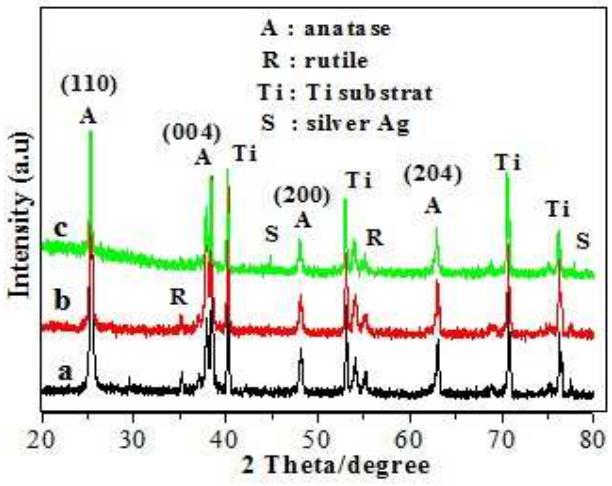

Fig. 1 XRD patterns for samples of TiO_2 (a), N-TiO_2 (b) and Ag/N-TiO_2 (c)

The peaks belonging to Ti substrate can be clearly found for all samples, which confirms that synthesis of nanotube arrays TiO_2 on the Ti substrate was successful. For the Ag/N-TiO_2 after electrochemical deposition treatment for 10 s, two weak peaks at 44.3° and 77.2°, attributed to the characteristic peaks of Ag (200) and (220) are observed (Fig.1c), indicating that the N-TiO_2 nanotube arrays surface was deposited with Ag nanoparticles, which is consistent with early reported [21]. For all samples gave similar peaks, which may be implied that the crystalline structure are not altered after N doping into TiO_2 lattice, and Ag-deposit on the nanotubes arrays surface.

The FESEM images of the top view and the cross-sectional (inset image) of N-TiO_2, respectively are shown in Fig. 2a. As shown in Fig. 2a, the morphology of N-TiO_2 are opened at the top with an average diameter of 65 nm and wall thickness to be 15 nm. The cross-sectional image of the N-TiO_2 shown the nanotube arrays are vertical to the Ti substrate and its tube length is approximated to 900 nm.

The as-prepared N-TiO_2 nanotube arrays would be further modified by Ag deposition. Fig. 2b shows the top views of Ag/N-TiO_2 with the deposition time of 10 s at a constant direct potential of 1.0 V. Some Ag nanoparticles on the top of N-TiO_2 nanotubes are observed. However, the size of Ag nanoparticles is not clearly seen in the FESEM image. The detailed information of Ag is determined by TEM measurement. The TEM image of N-TiO_2 decorated with Ag is illustrated in Fig.2c. It is clear that the deposited Ag nanoparticles with the diameter of around 20-30 nm (shown in circles) dispersed uniformly over the surface of N-TiO_2 nanotube arrays.

The composition (atomic %) of the N-TiO_2 and Ag/N-TiO_2 are investigated by energy dispersive X-ray spectroscopy (EDX), as shown in Fig. 3. It can be seen that the Ag/N-TiO_2 sample consist of five elements, with an atomic ratio (%) of O, Ti, N, C, and Ag are 63.41, 27.61, 3.35, 3.36 and 2.15 %, respectively. It is clear that the Ag nanoparticles deposited on the surface of N-TiO_2 nanotube arrays.

The overall chemical composition of the as-prepared TiO_2 and Ag/N-TiO_2 were determined by XPS, as shown in Fig. 4a-d. Fig. 4a shows that the XPS spectrum of N 1s region for Ag/N-TiO_2 appears at 400.6 eV is typical for N-TiO_2 [11].

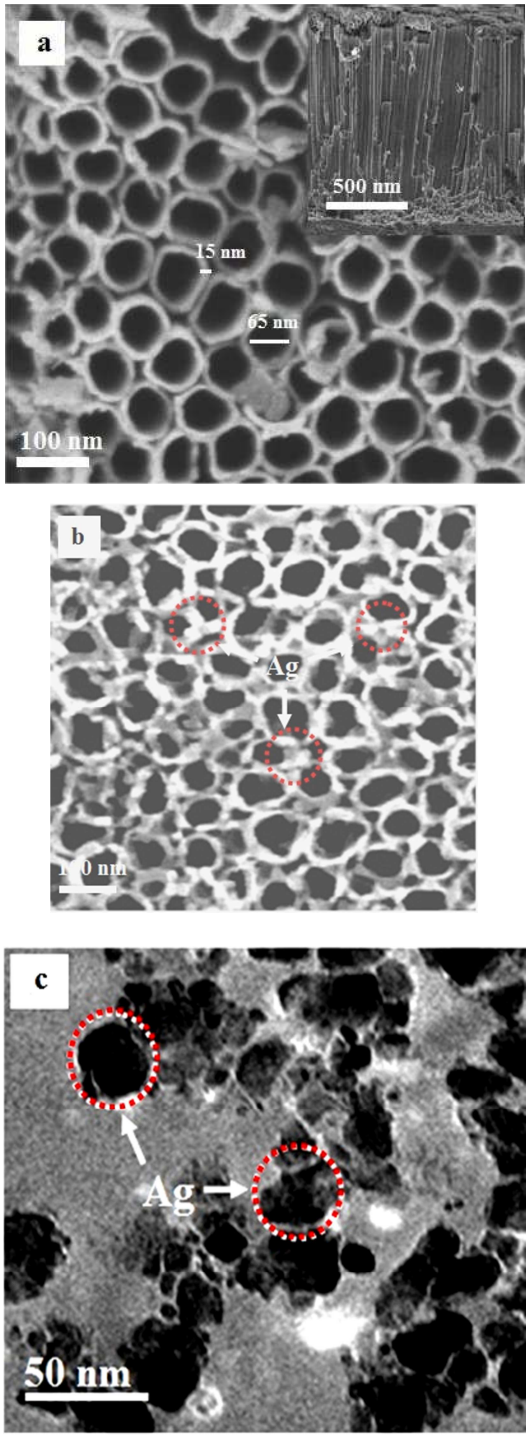

Fig. 2 (a) FESEM images of N-TiO_2 , (b) Ag/N-TiO_2 and (c) TEM image of top view of Ag/N-TiO_2 after deposition time for 10 s with potential of 1 V

According to the earlier studies [12], [15], [25], this N 1s peak at around 400.0 eV can be attributed to the oxidized nitrogen in the form of N-Ti-O linkage, namely interstitial N. The electronegativity of N doped into TiO_2 lattice is lower than O element, leading to reducing of electron density on the N [26]. This result indicates that calcining process indeed leads to substitution of N atoms for O sites in TiO_2 lattice. This deduction can be further investigated by Ti 2p spectra. In Fig. 3b, the Ti $2p_{3/2}$ and $2p_{1/2}$ core level peaks of Ag/N-TiO_2 appear at 458.9 eV and 464.9 eV, respectively. They shift to lower binding energy by 0.3 eV compared with TiO_2.The redshift may be implied a higher electron density and might be attributed to the doping of N into TiO_2 lattice [18], [24], [26]. The O 1s XPS spectrum in Fig. 3c can be separated to two peaks at 530.2 and 531.6 eV, respectively, further confirming the formation of the N-Ti-O structure, which is consistent with the early reported N-doped TiO_2 [12], [24], [26]. These results suggest that the TiO_2 lattice is considerably modified by interstitial N for the prepared Ag/N-TiO_2 nanotube arrays. Fig. 4d shows the XPS spectrum of Ag 3d consist of two peaks at around 368.6 eV and 374.6 eV, respectively attributed to Ag $3d_{5/2}$ and $3d_{3/2}$ region, consistent with reported by Sun et al. [18]. The splitting of 3d orbital of Ag with energy separation of 6.0 eV, indicates that the deposited Ag mainly exists in the Ag^o state on the N-TiO_2 nanotube surface [24], [27].

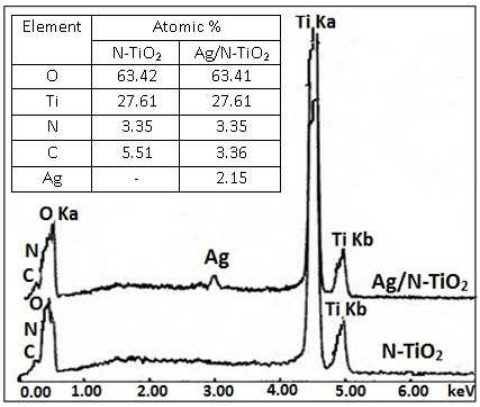

Fig. 3 EDX spectra of N-TiO_2 and Ag/N-TiO_2 obtained after deposition for 10 s and inserted table of atomic composition

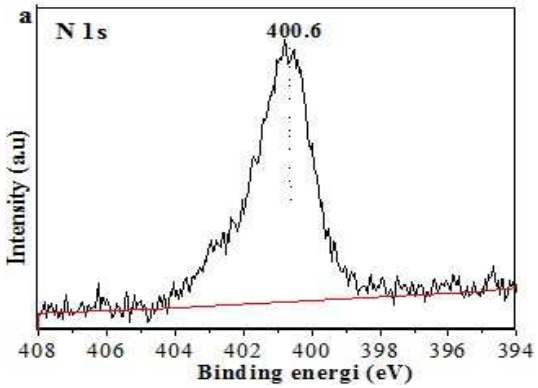

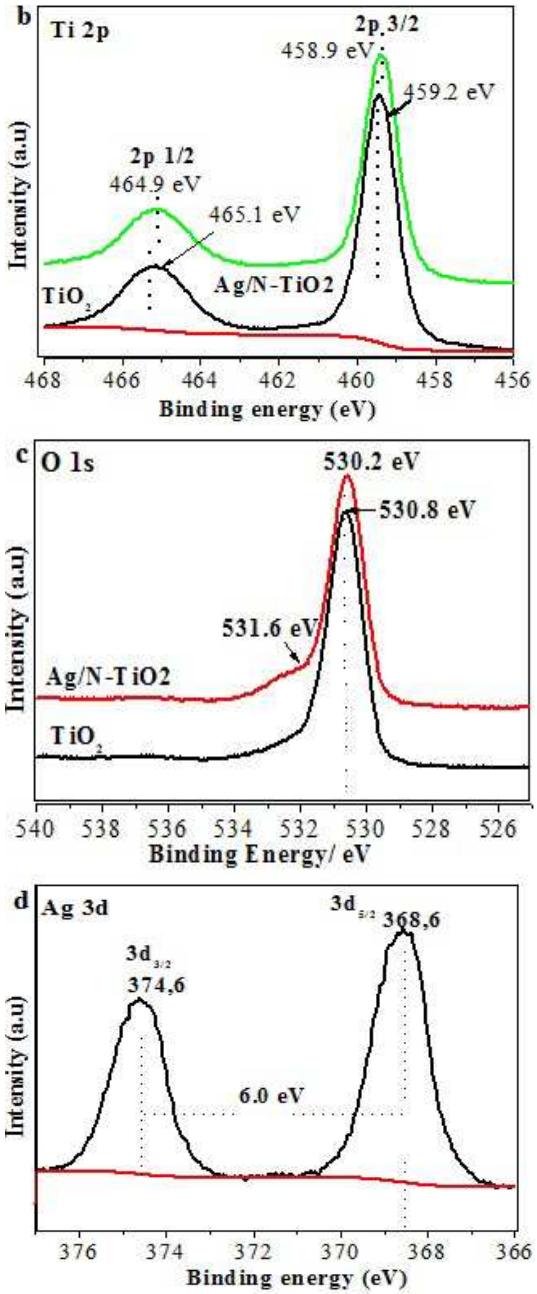

Fig. 4 (a) High-resolution XPS spectra of N 1s region; (b) Ti 2p; (c) O 1s and (d) Ag 3d of the Ag/N-TiO_2 obtained

Fig. 5 shows the UV-visible absorption spectra of TiO_2, N-TiO_2 and Ag/N-TiO_2 samples. For the undoped TiO_2 exhibits absorption in a wavelength region below 400 nm is due to the intrinsic interband transition absorption of anatase TiO_2 (curve a), while the absorption edge of N-TiO_2 is red shift toward visible light region around 400 nm (curve b). It indicates that the doping of N into the TiO_2 lattice have been successful. Compared with the TiO_2 and N-TiO_2, the optical absorption edge of Ag-TiO_2 and Ag/N-TiO_2 extend to the visible light region.

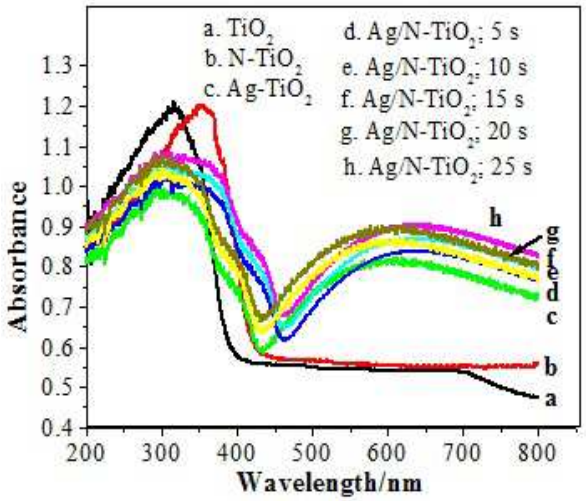

Fig. 5 Absorption UV-visible spectra of TiO_2, N-TiO_2, Ag-TiO_2 and Ag/N-TiO_2 after deposition Ag for (5-25 s)

As can be seen, the absorption broad peaks around 450 nm (curve c-h). The red-shift might be related to the interaction between TiO_2 and Ag particles, which is contributed to surface plasmon induced photoexcited electrons of Ag nanoparticles [25], [28]-[29]. It was found that the optical absorption of Ag/N-TiO_2 is strongest after deposition time for 10 s (curve e). However, as the deposited time increases upper 10 s, the absorption band edges of Ag/N-TiO_2 are blue-shift (curve f-h). These may be indicated that the Ag nanoparticles size increases. The plasmonic of Ag nanoparticles have provided enhanced property by scattering and hot electrons transfer process [29]. Generally, the scattering process would occur at nanoparticles with a size of 100 nm [25], [30]. Among all synthesized samples, the Ag/N-TiO_2 after deposited for 10 s exhibits the best visible light absorption, consistent with FESEM image which is the Ag-nanoparticles with a diameter of around 20-30 nm have been dispersed over the surface of N-TiO_2 nanotube arrays.

The Ag nanoparticles can strongly interact with visible light owing to plasmonic resonance, which is enhanced the light absorption and charge separation. Localized plasmon resonance (LPR) effects of plasmonic Ag contribute to the charge separation via the electrons and plasmon resonance energy transfer [29].

The linear sweep photovoltammetry methods were carried out to investigate the photoelectrochemical properties of Ag/N TiO_2 electrode. Fig. 6 shows the linear sweep voltammograms (LSV) of different samples in KOH (0.1 M) as electrolyte under visible light irradiation with the same experimental conditions.

Generally, as well known that the TiO_2 is not a response to visible light, but in our work shows very low photocurrent (curve b), because the halolite lamp as used as the visible light source contains UV light a portion of 10%. The photocurrent density of N-TiO_2 is much higher than that of TiO_2, where arise to 0.52 and 0.02 mA.cm^{-2}, respectively. This is an indication that the formation of photogenerated electron-hole pairs on the surface of N-TiO_2 is easier to occur than TiO_2 when absorbing visible light because it has a smaller band gap as a result of the mixing of the N 2p orbitals with O 2p [11]. In comparison with TiO_2 and N-TiO_2, the Ag-TiO_2 shows higher photocurrent responses of 0.58 mA.cm^{-2}

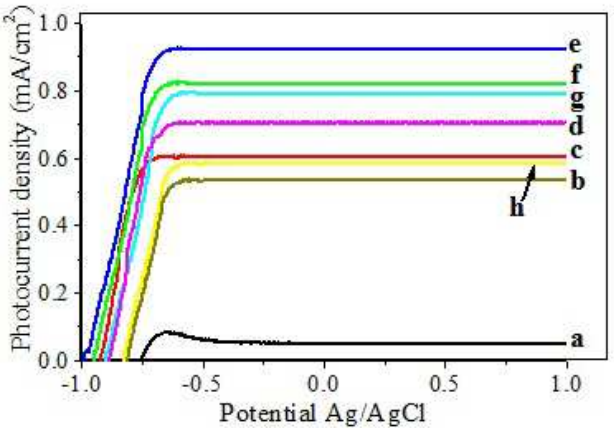

Fig. 6 Linear sweep voltamograms of: (a) TiO_2, (b) N-TiO_2, (c) Ag-TiO_2, (d) Ag/N-TiO_2 electrode after deposited for 5 s, (e) 10 s, (f)15 s, (g) 20 s and (h) 25 s, in KOH 0.1 M under visible light irradiation

For Ag nanoparticles are deposited on the N-TiO_2 surface with deposition time for 5 s, and 10 s, the photocurrent density of Ag/N-TiO_2 increased 0.67 and 0.92 mA.cm^{-2}, respectively as shown in Fig.5 consistent with the absorption spectra. However, the deposition time increased to 15, 20 and 25 s, the photocurrent density of Ag/N-TiO_2 decrease to 0.79, 0.77 and 0.56 mA.cm^{-2}, respectively. As can be seen, the photocurrent densities of Ag/N-TiO_2 with deposition time for 10 s are highest all among electrodes. These results indicate that lower recombination of photogenerated electron-hole pairs due to the Schottky barriers formed at the interface between Ag nanoparticles and N-TiO_2 [31]. Furthermore, the photogenerated electron easily transfers from Ag/N-TiO_2 to counter electrode via external circuit [23], [25].

It can be seen in Fig. 6 that the zero-current potential (Ezcp) for the Ag/N-TiO_2, N-TiO_2, and TiO_2 were -0.10 V, -0.86 V and -0.75 V, respectively. Compared to the TiO_2, the Ezcp for the Ag/N-TiO_2 appears the negative shift about 0.25 V. It may be ascribed to the Ag/N-TiO_2 need a lower potential to transfer the photogenerated electrons to an external circuit. These results are consistent with the absorption spectra, thus contributing the synergistic effect of N-doping and Ag nanoparticles. Obviously, the N-doping into TiO_2 lattice narrowed the band gap energy and improved the optical absorption visible light. The Ag nanoparticles are deposited on the N-TiO_2 surface not only extend the absorption range due to its SPR but also facilitate the separation of photogenerated electron and hole, which is beneficial to improve the photocatalytic efficiency under visible light irradiation.

Degradation of methylene blue (MB) experiments were carried out to evaluate the photocatalytic (PC) activities of the obtained electrode, under visible light irradiation. The effect of deposition time on PC activity was investigated, as shown in Fig. 7a. After Ag nanoparticles deposited for 5 s formed Ag/N-TiO_2, the MB was degraded 54% under visible light irradiation for 240 min. When deposition time increases

to 10s, degradation ratio of MB increase about 69% and then decreases with the further increase of the deposition time.

The optimum deposition time is 10 s that the Ag nanoparticles with the diameter approximately of 20-30 nm are dispersed uniformly on the top of N-TiO_2 nanotube arrays (as shown Fig. 2b). The increasing of the size of the Ag nanoparticles is responsible for increasing degradation efficiency. While the deposited time increases upper 10 s, the degradation ratio of MB is decreased, which consistent with FESEM and photocurrent response. It may be indicated that a bigger Ag nanoparticle was deposited on the surface of the N-TiO_2. The optimum deposition time results in the fastest degradation rate of MB, which consistent with the absorption spectra and photocurrent response in the visible light region. In addition, the conglomeration of Ag was deposited on the N-TiO_2 surface would decrease the active site of N-TiO_2 to contact with MB molecules and hinder of the N-TiO_2 surface from absorbing visible light [17].

The PC degradation of MB in aqueous solutions was performed on TiO_2, N-TiO_2 and Ag/N-TiO_2 electrode under visible light irradiation, as shown in Fig. 7b. It can be seen in Fig. 7b that the TiO_2 have a low PC activity with only 9% of the MB degraded within 240 min. The PC activity of the N-TiO_2 is higher than the TiO_2 electrode, can degrade MB about 48%. It may be ascribed to the improved the optical absorption visible light by N-doping.

In contrast, the Ag/N-TiO_2 electrode after deposition time for 10 s demonstrated a highest PC activity than all electrodes can degrade MB over 68%. This suggests that simultaneous integration of N-doping and Ag-depositing due to its SPR which is extended the absorption range can synergistically improve the photocatalytic performance of TiO_2. Moreover, the interaction between N-TiO_2 and Ag nanoparticles interface formed barrier Schottky as trapped photogenerated electron which beneficial to enhance the photocatalytic efficiency.

Comparison of MB degradation by different PC and photo-electro-catalytic (PEC) processes under visible light irradiation is performed on the obtained electrodes, as shown in Fig. 7b. For all PEC process was applied an external anodic potential of 0.2 V and results in the MB degradation ratio on TiO_2, N-TiO_2, and Ag/N-TiO_2 electrodes about 14%, 57%, and 92%, respectively. The Degradation ratio (%) of the MB showed noticeable differences, where the PC is lower activity than PEC process.

The kinetic behavior of PC and PEC degradation of MB can be explained by the following Langmuir-Hinshelwood (L-H) equation [22], [32]:

$$\ln \frac{Co}{Ct} = -k.t \qquad (1)$$

where *Co* is the initial concentration, *Ct* is the remaining concentration of MB at the reaction time (*t*), and *k* is the apparent rate constant of pseudo-first-order (min^{-1}), respectively.

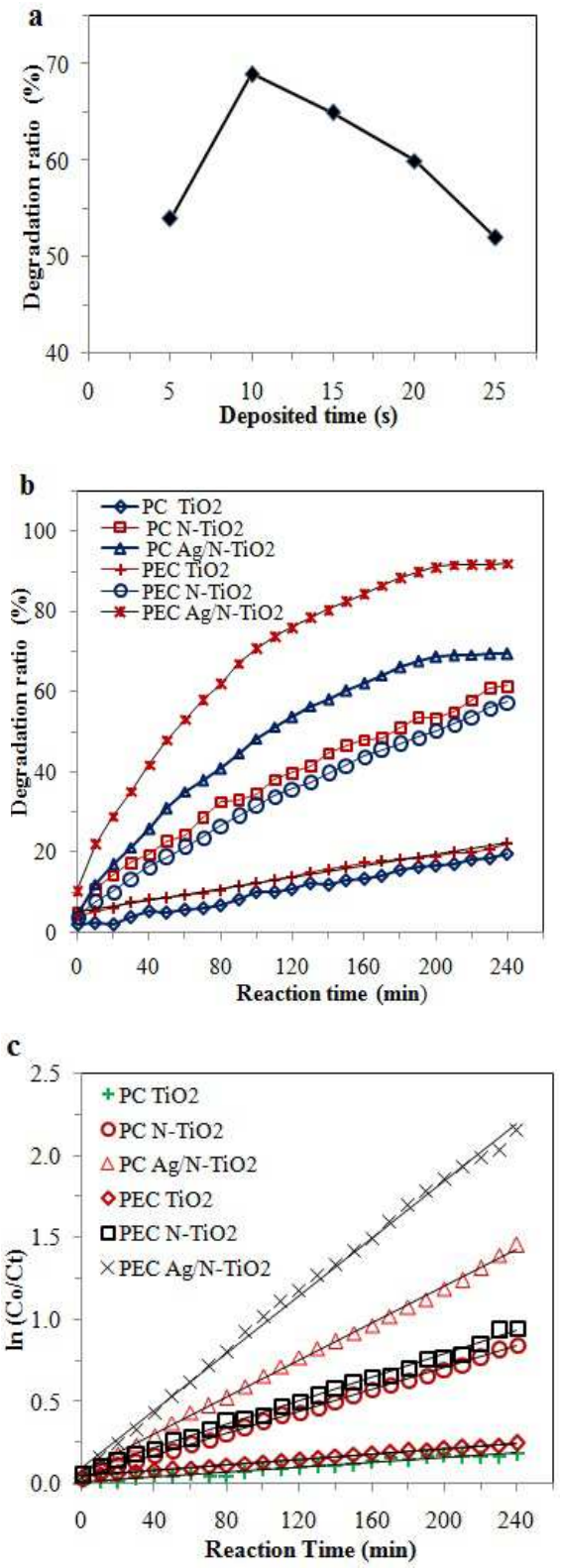

Fig. 7 (a) The PC degradation of MB on the electrode of deposited Ag by different time; (b) The PC and PEC process and (c) comparison of kinetic curves of MB by different processes on TiO_2, N-TiO_2 and Ag/N-TiO_2 electrode under visible light irradiation and bias potential applied 0.5 V

The comparison kinetic (ln *Co/Ct*) curves as a function of the reaction time of PC and PEC degradation of MB are performed on the different electrodes, are shown in Fig. 7c. The PEC degradation of MB clearly followed the first-order

reaction kinetics. The corresponding kinetic constants (*k*) of MB degradation are given in Table 1.

TABLE I
THE KINETIC CONSTANTS OF MB DEGRADATION BY DIFFERENT PROCESS ON TIO2, N-TIO2 AND AG/N-TIO2 ELECTRODE UNDER VISIBLE LIGHT IRRADIATION

Degradation Process	**Apparent rate constant, k (min^{-1})**		
	TiO_2	**N-TiO_2**	**Ag/N-TiO_2-10s**
PC	$5x10^{-4}$	$3x10^{-3}$	$6x10^{-3}$
PEC	$1x10^{-3}$	$4.5x10^{-3}$	$9x10^{-3}$

It can be seen that the PEC degradation MB are faster kinetics than PC for all electrodes because the bias potential is driving photogenerated electron to counter electrode via an external circuit. When the bias potential of 0.5 V is applied to TiO_2 electrode, PEC degradation rate of MB is approximately 2.0 times of PC degradation rate using the same electrode. For N-TiO_2 electrode, PC and PEC degradation rate of MB are 6.0 and 4.5 times of that the TiO_2. Obviously, the Ag/N-TiO_2 electrode shows the highest PEC degradation rate, being 9 times and 2 times larger than that the TiO_2 and N-TiO_2 electrode, respectively. These results ascribe that bias potential to the more effective separation of the photogenerated electron-hole pairs, which improved the photocatalytic efficiency [32].

We suggest that the N-doping into the TiO_2 lattice is more effective to improve the optical absorption visible light due to its narrowed the band gap, promote the excitation of electron-hole [11], [24]. The Ag nanoparticles decorated on the N-TiO_2 surface can extend the absorption edge to the visible light region due to its SPR leads to the improvement of photocatalytic activity.

When the surface of the Ag/N-TiO_2 electrode irradiated with visible light, the valence band electron (e^-) of N-doping are excited to the conduction band of TiO_2. After Ag nanoparticles are decorated on the TiO_2 surface, and the Schottky barriers are formed in the interface region between Ag nanoparticles and N-TiO_2 [22]. The photogenerated electrons are trapped by Schottky barriers and then rapidly transferring them to the adsorbed O_2 on the surface of TiO_2 to form highly oxidative species such as $O_2^{\bullet-}$**,** which can further initiate the degradation reaction of MB [23]. Simultaneously, the photogenerated hole (h^+) could either recombine with electron or react with OH^- or H_2O to form radical hydroxyl radical $^{\bullet}OH$ [22], [24]. The generated $^{\bullet}OH$ and $O_2^{\bullet-}$ are responsible for the degradation of MB. In this work, the recombination of the photogenerated electron and hole pairs are depressed by the external electric field. The lower recombination rate of photogenerated electron and hole of Ag/N-TiO_2 leads to the enhancement PEC degradation of MB. The photogenerated electrons are forced to transfer to the counter electrode via external circuit by applying an anodic bias potential about 0.5 V to the Ag/N-TiO_2 surface as the working electrode. While. the Schottky barriers in the interface region of the N-TiO_2 and Ag nanoparticles and potential gradient both can efficiently promote the separation of photogenerated electrons and holes, resulting in the enhancement of the photoelectrocatalytic activity. The oxygen absorbed on the surface of the counter electrode was reduced by a photogenerated electron to form $O_2^{\bullet-}$. Accumulation of photogenerated holes on the surface electrode led to the production of the $^{\bullet}OH$ [22], which was responsible for the PEC degradation of MB.

Overall, the enhancement of PEC activity of Ag/N-TiO_2 electrode can be attributed to three aspects. Firstly, N-doping into TiO_2 lattice can improve the visible absorption light due to decrease the band gap by mixing of N 2p states with O 2p states [11]. Secondly, the Ag nanoparticles were decorated on the N-TiO_2 surface can extend the absorption edge to visible light region due to its SPR. Moreover, interaction the N-TiO_2 and Ag nanoparticles interface formed barrier Schottky as trapped photogenerated electron which inhibits the of the photogenerated electron-hole pairs recombination [22]. Thirdly, bias potential applied is forced to transfer the photogenerated electron to the counter electrode via an external circuit, which is beneficial to enhance the photocatalytic efficiency.

IV. CONCLUSIONS

Highly dispersed Ag nanoparticles with a diameter of 20-30 nm were successfully deposited on the N-TiO_2 nanotube arrays by an electrochemical deposition method. The average inner diameter of the Ag/N-TiO_2 nanotubes was about 65 nm, the wall thickness of 15 nm and its length is approximately 900 nm. Compared with the TiO_2 nanotube arrays electrode, the Ag/N-TiO_2 electrode showed a significant enhancement PEC degradation of MB, was about 92% for 240 min under visible light irradiation. The kinetic constant of Ag/N-doped TiO_2 electrode was about 9 times higher than TiO_2. The enhanced photocatalytic activities under visible light irradiation of Ag/N-TiO_2 is a synergistic effect of N-doping and Ag nanoparticles. Furthermore, the kinetic constant PEC degradation of MB is contributed with photogenerated electron-hole separation efficiency, due to bias potential was applied to the surface electrode.

ACKNOWLEDGMENT

The author's acknowledgment was partly funded by the cluster research scheme from University of Indonesia [Titania photoelectrocatalysis (TiPEC)], contract number (1864/UN2.R12/HKP.05.00/2015) and PSPS-DGHE Bilateral Exchanged. Also, thank Mrs. Aminah and KAIS University for the spectroscopy measurement.

REFERENCES

[1] M.M. Jan, T. Hiroaki, G. Andrej and S. Patrik, "Dye-Sensitized anodic TiO2 nanotubes," Electrochem.Commun, vol. 7, pp. 1133, 2005.

[2] M.K. Gopal, S. Karthik, P. Maggie, V.K. Oomman and G.A. Craig, "Use of Highly-ordered TiO2 Nanotubes Arrays in Dye Sensitizer Solar Cells," Nano Lett , vol. 6, pp. 215-218, 2006.

[3] P. Maggie, M.K. Gopal, S. Kartik and G.A. Craig, "Visible Light Photoelectrochemical and Water-Photoelectrolysis Properties of Titania Nanotube Arrays," J. Photochem. Photobiol. A: Chemistry, vol. 178, pp. 8-15, 2006.

[4] P. Lily, E.L. Matthew, L.J. Thomas, G.A. Craig dan D.A. Tejal, "The Effect of TiO2 Nanotubes on Endothelial Function and Smooth Muscle Proliferation," Biomaterials, vol. 30, (7), pp. 1268-1272, 2009.

[5] L. Zhaoyue, Z. Xintong, N. Shunsuke, J. Ming, T.A. Donald, M Taketoshi and F. Akira, "Highly ordered TiO2 Nanotube Arrays with

Controllable Length for Photoelectrocatalytic Degradation of Phenol," J. Phys. Chem. C. vol. 112, pp. 253-259, 2008.
[6] S. Yaling, Z. Xingwang, Z. Minghua, H. Song and L. Lecheng, "Preparation of High efficient photoelectrode of N,F-codoped TiO2 nanotubes," J. Photochem. Photobiol A, vol. 194, pp. 152-160, 2008.
[7] L. Jingyuan, L. Na, Q. Xie, C. Shuo and Z. Huimin, "Facile Method for Fabricating Boron-Doped TiO2 Nanotube Array with Enhanced Photoelectrocatalytic Properties," Ind. Eng. Chem. Res, vol. 47, pp. 3804-3808, 2008.
[8] Ratnawati, G. Jarnuzi, D.L. Eniya, Slamet, "Effect of NaBF4 Addition on The Anodic Synthesis of TiO2 Nanotube Arrays Photocatalyst for Production of Hydrogen from Glycerol-Water Solution," International J. of Hydrogen Energy, vol. xxx, pp. 1-9, 2014.
[9] S.W. Seung, L.Y Jeong, A.S.Kwang, K.H. Soon and K.H. Jin, "Visible Light Absorbing TiO2 Nanotube Arrays by Sulfur Treatment for Photoelectrochemical Water Splitting," J. Phys. Chem. C, vol. 119 pp. 13375-13383, 2015
[10] C.X. Dong, A.P. Xian, E.H. Han and J.K. Shang, "C-Doped TiO2 with Visible Light Photocatalytic Activity," Solid State Phenomena, vol. 121, pp. 939-942, 2007
[11] A. Ryoji, M. Takeshi, O. Takeshi, A. Koyu and T. Yasunari, "Visible-Light Photocatalysis in Nitrogen-Doped Titanium", Science, vol. 293, pp. 269-271, 2001.
[12] L. Shipu, L. Shiwei, L. Jianjun, P. Nenqian, L. Danhong and L. Jianbao, "Nitrogen Doped TiO2 Nanotubes Arrays with Enhanced Photoelectrochemical Property," International Journal of Photoenergy, vol. 1, pp. 794207-794214, 2012
[13] L. Heping, Z. Wei, H. Siya and P. Wei, "Enhanced Visible-Light-Driven Photocatalysis of Surface Nitrided Electrospun TiO2 Nanofibers," Nanoscale, vol. 3, pp. 801-806, 2012.
[14] Y. Guotian, Z. Min, H. Jian and Y. Jianjun, "Photoelectrochemical and Photocatalytic Properties of N + S co-doped TiO2 Nanotube Array Films under Visible light irradiation," Mater. Chem. Phys, vol. 129, pp. 553-557, 2011.
[15] A.B. Anthoni, S. Hedi, K.K. Yuni and G. Jarnuzi, "Photoelectrocatalytic Performanced of Highly Ordered Nitrogen Doped TiO2 Nanotubes Array Photoanode," IOP Mater. Eng, vol. 172, pp. 012005-012015, 2017.
[16] C. Ye, T. Baozhu and Z. Jinlong, "Improving The Thermal Stability and Photocatalytic Activity of Nanosized Titanium Dioxide via La3+ and N co-Doping," Appl. Catal. B, vol. 101, pp. 376-381, 2011.
[17] Z. Jinlong, W. Yongmei, X. Minyang, L.K. Sajjad and S. Shamaila, "Development of modified N doped TiO2 photocatalyst with metals, nonmetals and metal oxides," Energy Environ. Sci., vol. 3, pp. 715-726, 2010.
[18] S. Hongqi, Z. Guanliang, L. Shizhen, A.M. Ha, T.O. Moses and W. Shaobin, "Visible Light Responsive Titania Photocatalysts co-doped by Nitrogen and Metal (Fe, Ni, Ag, or Pt) for Remediation of Aquaeous Pollutants," J.Chem. Eng, vol. 231, pp. 18-25, 2013.
[19] Z. Huarong, T. Keqi, Z. Haiwu, G. Yuzong and W.F. Zhang, "Preparation, Characterization and Photocatalytic Activity of TiO2 co-doped with Ytrium and Nitrogen," Mater. Chem. Phys, vol. 125, pp. 156-160, 2011.
[20] L. Yang, W. Xiaolei, Y. Fan and Y. Xiurong, "Excellent antimicrobial properties of mesoporous anatase TiO2 and Ag/TiO2 composite films," Microporous and Mesoporous Mater, vol. 114, pp. 431-439, 2008.
[21] J. Jiqing, W. Xiao, W. Frank, H. Anke, C. Liuping, F.V. Failla, M.J. Alfred and Z. Dai, "Polarization-Dependent SERS at Differently Oriented Single Gold Nanorods," ChemPhysChem, vol. 13, pp. 952-958, 2012.
[22] X. Kunpeng, S. Lan, W. Chenglin, L. Yuekun, W. Mengye, C. Hongbo and L. Changjian, "Photoelectrocatalytic Properties of Ag Nanoparticles Loaded TiO2 Nanotube Arrays Prepared by Pulse Current Deposition," Electrochimica Acta, vol. 55, pp. 7211-7218, 2010.
[23] S. Mingxuan, F. Yalin, S. Shanfu and W. Ying," Surface co-Modification of TiO2 with N Doping and Ag Loading for Enhanced Visible Light Photoactivity," The Royal Society of Chemistry, vol. 6, pp. 12272-12279, 2016.
[24] Z. Shenseng, P. Feng, W. H, Y Hao, Z. Shanqing, Y. Jian and Z, Huijun, "Electrodeposition Preparation of Ag loaded N-doped TiO2 Nanotube Arrays with Enhanced Visible Light Photocatalytic Performance," Catalysis Communications, vol. 12, pp. 689-693, 2011.
[25] J. Jiqing, T. Jianguo, G. Wei, K. Daibin, T. Yexiang and C. Liuping Chen, "Plasmonic Silver Nanoparticles Matched with Vertically Aligned Nitrogen-Doped Titanium Dioxide Nanotube Arrays for Enhanced Photoelectrochemical Activity," Journal of Power Sources, vol. 274, pp. 464-470, 2015.
[26] X. Mingyang, Z. Jinlong and C. Feng, "New Approaches to Prepare Nitrogen-Doped TiO2 Photocatalysts and Study on Their Photocatalytic Activities in Visible Light", Applied Catalysis B: Environmental, vol. 89, pp. 563-569, 2009.
[27] F. Xiao, F. Jun, H. Xiaoyun, L. Enzhou, K. Limin, T. Chunni, M. Yongning, W. Huitong and L. Yinye, "Preparation and Characterization of Ag Deposited and Fe Doped TiO2 Nanotube Arrays for Photocatalytic Hydrogen Production by Water Splitting," Ceramics International, vol. 40, pp. 15907-15917, 2014.
[28] T. Ichiro, Y. Fumitake and H. Kouji, "Localized Surface Plasmon Resonance Sensing Properties of Ag/TiO2 Films," Chem. Letters, vol. 35, pp. 454-455, 2006.
[29] M. Zhou, J. Li, Z. Ye, C. Ma, H. Wang, P. Huo, W. Shi and Y. Yan, "Transfer Charge and Energy of Ag@CdSe QDs-rGO Core-Shell Plasmonic Photocatalyst for Enhanced Visible Light Photocatalytic Activity," ACS Appl Mater Interfaces, vol. 7, pp. 28231-28243, 2015.
[30] W.C. Scott, and T. Elijah, "Plasmonic Solar Water Splitting," Energy and Environ. Sci, vol. 5, pp. 5133 -5146, 2012.
[31] S. Zhichao, W. Jianjun, X. Fangfang, H.Q. Fu and D. Hanming, "Highly Effective Silver-Semiconductor Photocatalytic Composites Prepared by a Silver Mirror Reaction," *J. Phys. Chem. C*, vol. 112, pp. 15423-15428, 2008.
[32] L. Yanbiao, G. Xiaojie, Z. Baoxue, X. Bitao, L. Jinhua, D. Chaoping, B. Jing and C. Weimin, "Photoelectrocatalytic Degradation of Tetracycline by Highly Effective TiO2 Nanopore Arrays Electrode," J. of Hazardous Mater, vol. 171, pp. 678-683, 2009.